Blasse's Pandora's box

Dorenbos, Pieter

DOI
10.1016/j.omx.2021.100076

Publication date
2021

Document Version
Final published version

Published in
Optical Materials: X

Optical Materials: X 11 (2021) 100076

Contents lists available at ScienceDirect

Optical Materials: X

journal homepage: www.elsevier.com/locate/omx

Invited article

(INVITED)Blasse's Pandora's box

Pieter Dorenbos

Delft University of Technology, Faculty of Applied Sciences, Department of Radiation Science and Technology, Mekelweg 15, 2629 JB Delft, Netherlands

ARTICLE INFO

Keywords:
Bismuth luminescence
Quenching phenomena
Electron transfer

ABSTRACT

Upon his retirement from science Blasse wrote a paper (Blasse, J. Lumin. 72-74 (1997) 129) addressing unsolved problems in explaining luminescence phenomena of classical phosphors. He used the metaphor of Pandora's box. A box full of disaster that should remain closed. Yet, Blasse did open that box and therewith spread the unsolved problems over the luminescence community. Only the hope to solve those problems remained inside the box. Today, 25 years later, we will explore whether the hope has managed to provide answers. The unsolved problems related to the fundamental understanding of luminescence from WO_4^{2-}, VO_4^{3-}, Sb^{3+}, Bi^{2+}, Bi^{3+}, Cu^{+}, and Ce^{3+}. Here we will show how vacuum referred binding energy diagrams can explain or can help to explain Blasse's unsolved problems of 1997.

1. Introduction

In his 1997 paper [1] G. Blasse gave various examples of well-known luminescence phenomena for which a quantitative and often even a qualitative explanation was still lacking. It concerned; (1) The absence of Tb^{3+} emission in YVO_4. (2) The absence of Ce^{3+} emission in the simple oxides La_2O_3, Y_2O_3, and Lu_2O_3. (3) The red Bi^{2+} emission and its unexpected chemistry. (4) The charge transfer emission involving Bi^{3+} and Pb^{2+}, and in particular the origin of the yellow emission of Bi^{3+} in YVO_4. (5) The high efficiency of Sb^{3+} emission in $Ca_5(PO_4)_3(F,Cl)$ despite a 19.000 cm^{-1} large Stokes shift. (6) A dramatic decrease of the quenching temperature of the WO_4^{2-} emission in the sequence $CaWO_4$, $SrWO_4$, $BaWO_4$, but when one replaces a small fraction of W^{6+} by U^{6+} the quenching temperature of the red uranate emission increases.

Many if not all of the issues raised by Blasse relate to phenomena where charge transfer together with lattice relaxation plays a role. The absence of Tb^{3+} 4f-4f and Ce^{3+} 5d-4f emission deals with spontaneous electron transfer from the Tb^{3+} and Ce^{3+} excited state to the conduction band. The unexpected chemistry of Bi^{2+} relates to valence stability which is connected to reduction and oxidation, i.e., electron transfer. The charge transfer emission from Bi^{3+} and Pb^{2+}, the uranate emission, all deal about electron transfer from the host bands to a localized impurity ground state. Tungstate and vanadate emission is from electron transfer from the cation, i.e., an electron at the conduction band bottom formed by W and V d-orbitals, to the anion, i.e., a hole in the valence band.

Things can be clarified with the methods to construct vacuum referred binding energy (VRBE) schemes. In 2012 the chemical shift model was published [2] and a further refined model appeared in 2020 [3,4]. They exploit the systematics in the spectroscopic properties in going through the lanthanide series, and the models enable to determine the electron binding energy in all divalent and all trivalent lanthanide ground and excited states in a compound with respect to the vacuum level. In addition it provides a unique method to derive the binding energy at the top of the valence band and at the bottom of the conduction band [5] which then forms the stepping stone to derive VRBEs in the $6s^2$ cations Tl^{+}, Pb^{2+}, and Bi^{3+} [6,7], in the transition metal elements with one 3d, 4d, or 5d-electron [8], and in the $3d^n$ ($n > 1$) transition metals [9,10].

In this work we will present the VRBE schemes for the compounds and luminescence centers that were addressed in Blasse's paper. Most unsolved problems from Pandora's box can be explained quite well once we have knowledge on the electron binding energies in the various states of the luminescence centers with respect to that in the host bands. Some problems remain, and that is mostly related to unknown lattice relaxation and how that affects the wavefunction of initial and final states in the luminescence process.

2. Vacuum referred binding energy schemes

The electron binding energy in a lanthanide $4f^n$ or $4f^{n-1}5d$ multi-electron state or at the valence band (VB)-top or conduction band (CB)-bottom is defined as minus the energy needed to remove an electron from such state and bring it to a state where both potential and kinetic energy of the electron will be zero. This is defined as the vacuum level. A VRBE scheme then shows the binding energies in the divalent and trivalent lanthanide ground and excited states together

E-mail address: p.dorenbos@tudelft.nl.

https://doi.org/10.1016/j.omx.2021.100076
Received 7 June 2021; Received in revised form 23 June 2021; Accepted 26 June 2021
Available online 2 July 2021

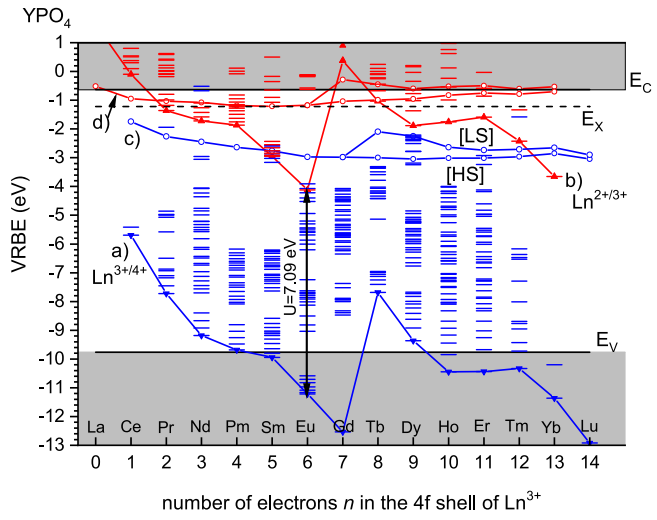

Fig. 1. The vacuum referred binding energy scheme for the trivalent and divalent $4f^n$ lanthanide ground state levels in YPO_4. (a) Connects the VRBE in the Ln^{3+} $4f^n$ ground state levels and can also be denoted as the $Ln^{3+/4+}$ charge transition level, (b) connects the same for divalent lanthanides, (c) connects the VRBE in the lowest energy $4f^{n-1}5d$ states of trivalent lanthanides where for $n > 7$ a distinction between the high spin [HS] and low spin [LS] states is made, (d) connects the same for divalent lanthanides. E_V, E_X, E_C are the VRBE at the valence band top, in the host exciton state, and at the conduction band bottom, respectively.

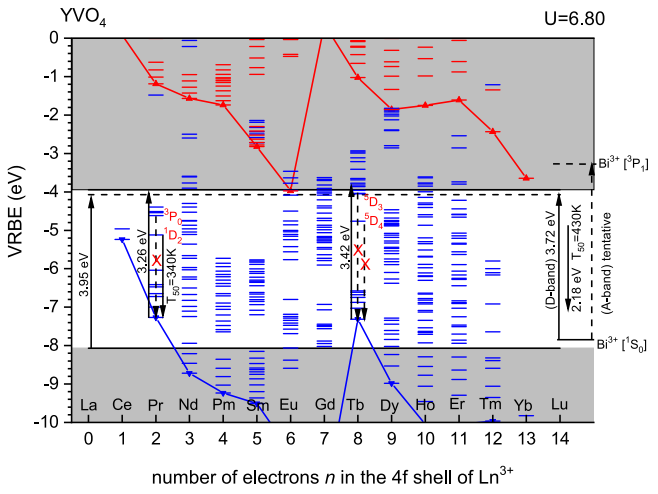

Fig. 2. The vacuum referred binding energy scheme for the divalent and trivalent $4f^n$ lanthanide levels in YVO_4 constructed using $U(6, A)$=6.8 eV and $\beta(2+, A) = \beta(3+, A)$=0.928. The location of the Bi^{3+} ground state and observed transitions (solid arrows) are also shown.

with that in the host bands. With the development of the chemical shift model in 2012 [2] and its further refinement in 2020 [3,4] we are able to construct such schemes routinely with sufficient accuracy to explain and predict many lanthanide luminescence phenomena.

The main physics behind the chemical shift model is a screening of the positive charge of the lanthanide by the surrounding chemical environment. An Ln^{2+} will be effectively screened by −2e of negative charge and an Ln^{3+} by −3e of negative charge. Screening is most optimal in a metal environment where the free conduction band electrons can approach the lanthanide most closely. Screening is least optimal in a fluoride compound where electrons are strongly bonded in the $2p^6$ fluorine orbitals. In between, screening scales with how strong electrons are bonded in the anion which in turn follows the familiar nephelauxetic sequences, i.e, $F < O < Cl < Br < N < I < S < Se$ and within the oxides $SO_4^{2-} < CO_3^{2-} < PO_4^{3-} < H_2O < BO_3^{3-} < SiO_4^{4-} <$ *aluminates* $< RE_2O_3$ [11]. The Coulomb repulsion between the negative screening charge with an electron in the lanthanide causes a reduction in the lanthanide electron binding energy. This reduction is called the chemical shift and is by definition zero for the electron binding energy in the free and unscreened lanthanide ions.

Over the years YPO_4 has served as a model compound to develop, to test, and to refine the chemical shift model, and a diversity of techniques has been applied to obtain data on energy level locations. Fig. 1 shows the VRBE diagram for YPO_4. It was obtained with the refined chemical shift model and the diagram can also be found in [4]. The most important parameter in diagram construction is the Coulomb repulsion energy $U(6, A)$. It is defined as the binding energy difference between an electron in the Eu^{2+} ground state with that of an electron in the Eu^{3+} ground state in chemical environment A. Its value can be deduced from spectroscopic data, and provides the crucial link between a host referred binding energy diagram (HRBE) and a VRBE. $U(6, free)$ is 18.05 eV for free europium ions and varies from 7.6 eV in highly ionic fluoride compounds (strong anion electron bonding) down to ≈6.0 eV in highly polarizable sulfide and selenide compounds (weak anion electron bonding). The smallest value of about 5.7 eV applies for Eu metal with free conduction band electrons. For YPO_4 a value of 7.09 eV applies.

In the refined chemical shift model of 2020, the nephelauxetic effect on the binding energy in the lanthanide $4f^n$ ground state was included, and parameters $\beta(Q, A)$ (Q = 2+ or 3+) were added to the model. It turns out that the binding energy for $n \geq 8$ may increase (becomes more negative) several 0.1 eV due to the nephelauxetic effect. The effect for $n \leq 7$ is quite insignificant and hardly to notice experimentally. The schemes and VRBE data presented in this work were all obtained with the refined chemical shift model.

3. Blasse's unsolved problems

3.1. The absence of Tb^{3+} 4f-4f emission in YVO_4

One of Blasse's unsolved problems was the absence of Tb^{3+} 4f emission in YVO_4. Blasse already suspected that charge transfer from the excited $^5D_3$ and $^5D_4$ Tb^{3+} states to V^{5+} plays a role in this [1]. Due to the work by Boutinaud et al. [12,13] on inter valence charge transfer (IVCT) involving Pr^{3+} and Tb^{3+} in many different types of compounds the issue was basically solved to be further confirmed with VRBE scheme construction. In [14] VRBE schemes for the lanthanides in vanadates, titanate, molybdate, niobate, tungstate, and tantalate compounds were made employing IVCT data. The relation between the quenching temperature for $^3P_0$ Pr^{3+} emission and for the $^5D_3$ and $^5D_4$ Tb^{3+} emission with the level location in the bandgap was studied. Fig. 2 shows the VRBE scheme that applies to YVO_4.

The VRBE in the lowest $4f^{n-1}5d$-state of Pr^{3+} and Tb^{3+} in compounds is, with the refined chemical shift model, on average found at −2.0 eV and −2.7 eV. Whenever the CB-bottom is at lower VRBE, one may observe an IVCT band. The observed IVCT band energies of 3.26 eV and 3.42 eV for Pr^{3+} and Tb^{3+} in YVO_4 can then be added to the VRBEs in the Pr and Tb ground states as illustrated in Fig. 2. It provides the VRBE of about -4 eV at the CB-bottom formed by the empty 3d-orbital of V^{5+}. The energy difference between an excited $4f^n$ level with the CB-bottom then controls the quenching temperature, and there appeared a roughly linear relation [14]. The $^5D_3$ excited state of Tb^{3+} is near the CB-bottom and emission is fully quenched. The $^3P_0$ level of Pr^{3+} is still relatively close below the CB-bottom and quenching temperature is well below room temperature, the Pr^{3+} $^1D_2$ level is far enough below the CB-bottom and the red emission from this state is observed though with a low quenching temperature. At T_{50}=340 K luminescence intensity has decreased by 50% [13]. The absence of the $^5D_4$ emission from Tb^{3+} is now related with the low lying conduction band bottom at −4 eV leading to a quenching temperature that is well-below room temperature.

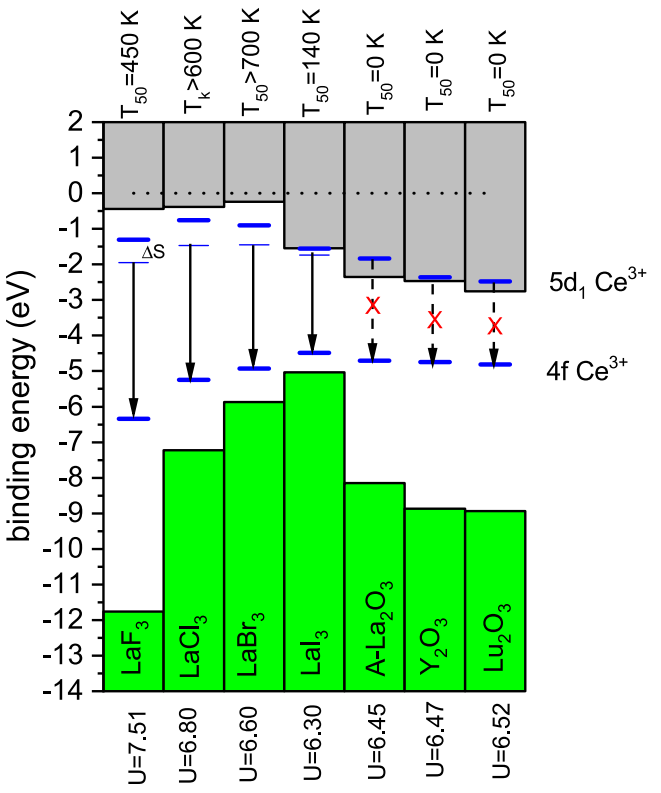

Fig. 3. Stacked diagram showing the VRBEs at the VB-top, the CB-bottom, in the Ce^{3+} ground state and in the lowest energy $5d_1$-state. The Stokes shift ΔS between excitation and emission is indicated. The quenching temperatures T_{50} for Ce^{3+} 5d-4f emission and the used value for $U(6, A)$ are shown.

3.2. The absence of Ce 5d-4f emission in the sesqui-oxides

As with the quenching of the Tb^{3+} and Pr^{3+} emission in the transition metal based compounds like YVO_4, the quenching of the Ce^{3+} 5d-4f emission is directly linked to the location of the lowest 5d-level with respect to the conduction band bottom. By means of photoconductivity experiments it was already found that the absence of Ce^{3+} emission in the simple oxides La_2O_3, Y_2O_3, and Lu_2O_3 is caused by a lowest 5d-level location inside the conduction band (see e.g. [15]). The VRBE in the lowest 5d-level of Ce^{3+} is on average near −1.6 eV and variations therein follow the size of the crystal field splitting [4,8]. This means that temperature stable Ce^{3+} 5d-4f emission can only be observed when the CB-bottom is well above −1.6 eV. This is the case for YPO_4 in Fig. 1 but not for YVO_4 in Fig. 2. Actually in all vanadates, titanate, molybdate, niobate, tungstate, and tantalate compounds, the CB-bottom is below −3 eV and Ce^{3+} emission is never observed [14].

Fig. 3 shows a stacked diagram with all four binary La-halide and three rare earth sesquioxide compounds. The $U(6, A)$ value determines the VRBE in the Ce^{3+} ground states. The lowest 5d-state of Ce^{3+} is above the average near −1.6 eV in compounds with small 5d crystal field splitting as in LaF_3, $LaCl_3$ and $LaBr_3$. Although crystal field splitting in the sesquioxides is large leading to relatively low VRBE in the 5d-state, the VRBE at the CB-bottom appears even lower which is the reason for the absence of Ce^{3+} emission in all rare earth sesquioxides. Ce^{3+} 5d-4f emission has been observed at low temperature in Lu_2O_3 when high pressure is applied [16]. Because of band gap widening the CB-bottom moves above the lowest 5d-level.

Blasse's unsolved problem for the absence of Ce^{3+} emission in the sesquioxides now boils down to answering why the CB-bottom is at such low VRBE. The states at the CB-bottom are formed by empty 5d (La and Lu) or 4d-states (Y) that are subject to similar crystal field splitting as the Ce^{3+} 5d-state. This is also the reason why the CB-bottom of d-electron nature tends to follow the VRBE in the 5d of Ce^{3+} as can be seen in Fig. 3. In addition to crystal field splitting we have to deal with the covalence (orbital mixing) between the rare earth and anion which tends to move the valence band up and conduction band downwards.

3.3. The red Bi^{2+} emission and its unexpected chemistry

Bi^{3+} is the preferred valence state in inorganic compounds but also Bi^{2+} can be stable and it then shows emission in the 600–700 nm spectral region [17,18]. Interest in Bi^{2+} has increased because of potential phosphor application in white-LEDs, and there is also active research in afterglow and storage phosphors where Bi^{3+} may act as a stable electron trapping and/or hole trapping center [19–22].

The VRBE energies in the Bi^{3+} and Bi^{2+} ground and excited states in compounds were determined by Awater et al. [6,23,24]. Fig. 4 shows a stacked VRBE diagram of pure bismuth compounds and compounds in which Bi^{2+} acts as emitting center or as an electron trap in thermoluminescence. The diagram is quite similar to the one that can be found in Awater et al. [23]. Slight differences are due to the use of the refined chemical shift model. Various methods to determine or estimate the VRBE in the $^2P_{1/2}$ ground state and emitting $^2P_{3/2}(1)$ excited state of Bi^{2+} were used [23].

On the left of the stacked diagram five pure Bi-compounds can be found. The VRBE data for BiF_3 with the VB-top at −9.6 eV is based on X-ray photoelectron spectroscopy (XPS) data from Poole et al. [25]. The $^5D_4$ excited state of Tb^{3+} is at −5.77 eV which is consistent with the quenching temperature of $T_{50}\approx300$ K from Back et al. [26]. In $NaBiF_4$ the $^5D_4$ Tb^{3+} level is near −5.66 eV with T_{50}=450 K [26]. For $BiPO_4$ the Eu^{3+} CT-band at 4.51 eV appears [27] just below the host exciton band and that was the basis to estimate the host band VRBE values. Bi_2O_3 is well-studied for photo-catalytic purposes [28–30] and the derived VRBE data are consistent with the observation of a Pr^{3+} IVCT band near 2.7 eV [31].

For the compounds 6 (SrF_2) until 15 ($Sr_2P_2O_7$), Bi^{2+} appears to be a stable valence and characteristic red Bi^{2+} emission has been reported. For the compounds 16 ($Li_2BaP_2O_7$) until 20 ($Y_3Al_5O_{12}$), Bi^{3+} is the preferred valence. Here Bi^{2+} was created by X-ray or β-irradiation of the Bi^{3+} doped sample. Bi^{2+} emission can then be observed in compounds 16 and 17 but for compounds 18 ($NaYGeO_4$) until 20 ($Y_3Al_5O_{12}$) luminescence is absent due to a low lying CB-bottom. Bi^{3+} acting as an electron trapping center was studied in YPO_4 by Lyu et al. [20] and Awater et al. [24], in $NaYGeO_4$ by Lyu et al. [21], in $Y_3Al_5O_{12}$ by Katayama et al. [19], and in $MgGeO_3$ by Katayama et al. [22]. Note that the ground state of Bi^{2+} in the oxides is near −3.5 eV to −4.0 eV and that for Bi^{3+} near -8 eV. That knowledge was used to estimate the VRBEs in the host bands of $Bi_4Ge_3O_{12}$ (compound 4). With the VB-top at −8.4 eV and CB-bottom at −3.6 eV, there is consistency with the bandgap of $Bi_4Ge_3O_{12}$.

With the knowledge on VRBEs, Blasse's problem of the unexpected chemistry of Bi^{2+} and its emission seems not to be a real problem. The VRBE in the ground state of Bi^{2+} changes from somewhat below -4 eV in the fluoride compounds towards the −3.5 eV region in the oxide compounds which is quite the same as the VRBE in Eu^{2+}. Bi^{2+} appears therefore about equally stable against oxidation as Eu^{2+}, and in that sense the chemistry of Bi^{2+} should not be too much different from that of Eu^{2+}.

Clearly, as with Eu^{2+} 5d-4f emission, the red emission from Bi^{2+} can only be observed when the VRBE at the CB-bottom is well above the VRBE in the excited Bi^{2+} $^2P_{3/2}(1)$ state. This is the case for compounds 6 until 17 in Fig. 4. In compounds 18 until 20 with low lying conduction band bottom, Bi^{2+} will be non-luminescent but it may still play a role in thermoluminescence whenever the Bi^{2+} ground state is below the CB-bottom. Bi^{3+} can then act as electron trapping center thus producing meta-stable non-luminescent Bi^{2+}. Upon electron release to the CB-band thermoluminescence can be generated. The temperature T_m at the

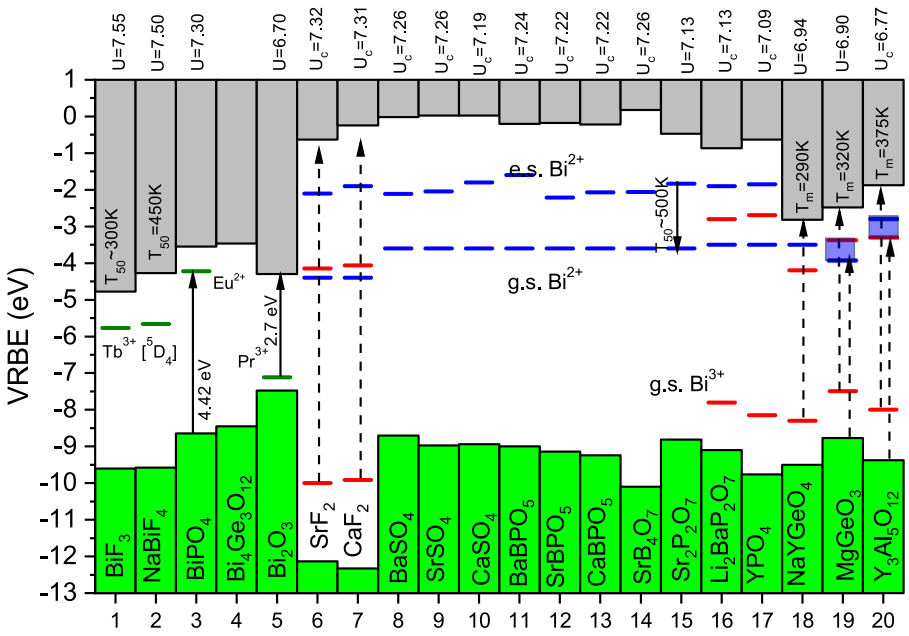

Fig. 4. Stacked diagram showing the VRBEs at the VB-top and the CB-bottom together with (sometimes tentative) Bi^{2+} and Bi^{3+} level locations. The used value for the U(6,A) parameter is provided at the top of the diagram. Bi^{3+} $^1S_0$ ground states (g.s.) and $^3P_1$ excited states (e.s.) are shown in red. The Bi^{2+} ground and excited states are shown in blue, and relevant Tb^{3+}, Pr^{3+} and Eu^{2+} states in green. Bi^{2+} g.s. level locations in compounds 18, 19, 20 were derived from thermoluminescence studies. Those for compounds 6 until 17 are just estimated positions keeping in mind an expected slightly more negative ground state VRBE with larger U-value.

maximum of the TL-glow peak for those compounds is shown in Fig. 4 and it was used to estimate the VRBE in the Bi^{2+} ground state. In case of $MgGeO_3$, a 4.86 eV charge transfer band [22] might be due to a Bi^{3+}→CB or VB→Bi^{3+} charge transfer. Both transitions are shown in Fig. 4. The Bi^{2+} ground state is then found at lower energy than when using the T_m value. Similar applies to $Y_3Al_5O_{12}$.

3.4. The charge transfer emission involving Bi^{3+} and Pb^{2+}

Bi^{3+} and Pb^{2+} are with the $6s^2$ electron configuration in the ground state iso-electronic, and in compounds they usually display the so-called A-band emission and A-band excitation due to transitions between the $^1S_0$ ground and $^3P_1$ excited state. The A-band energy scales with the $U(6, A)$ value. In other words it scales with how strong electrons are bonded in the anions. Based on charge (electron) transfer bands from VB→Bi^{3+} and Bi^{3+}→CB one may deduce the location of the Bi^{2+} or Bi^{3+} ground state inside the band gap of the host compound. The dashed arrows with compounds 6 (SrF_2), 7 (CaF_2), 18 ($NaYGeO_4$), 19 ($MgGeO_3$) and 20 ($Y_3Al_5O_{12}$) in Fig. 4 show observed CT-energies that were used to locate the Bi^{3+} or Bi^{2+} ground states. A systematic analysis comprising many different compounds with data retrieved from literature was done by Awater et al. [6]. Not only for Bi^{3+} but also for Pb^{2+} and Tl^+ [7]. Very clear systematics appears. The VRBE in the Bi^{3+} ground state increases from around −10 eV in fluorides to from −8 to −7 eV in oxide compounds and around −5 eV in iodide and sulfide compounds. A similar trend applies to Pb^{2+} and Tl^+.

The normal A-band emission can only be observed when the emitting $^3P_1$ level is located well below the CB-bottom. This is the case for compounds 6, 7, and 16 to 20 in Fig. 4. Whenever the CB-bottom is too close or even below, A-band emission is quenched to be replaced with what is known as charge transfer emission or D-band emission. The yellow 570 nm (2.18 eV) emission of Bi^{3+} in YVO_4 is now a clear case where the CB-bottom is located below the $^3P_1$ excited state. From the first report in 1971 by Boulon [32] and more recently by Krasnikov et al. [33], the Bi^{3+}→CB D-band in YVO_4 is found near 3.7 eV which upon excitation is followed by the strongly Stokes shifted 2.18 eV yellow emission. The transitions are shown on the right of Fig. 2 and position the Bi^{3+} ground state at VRBE≈-7.8 eV. The A-band excitation is to be expected near 4.5 eV which then would locate the excited $^3P_1$ state inside the conduction band at VRBE≈−3.3 eV.

Blasse also addressed the emission in the widely applied scintillator material $Bi_4Ge_3O_{12}$ that is characterized by a large Stokes shift. A-band emission was discarded already in 1997 and instead charge transfer (D-band) emission was proposed. The (tentative) $Bi_4Ge_3O_{12}$ VRBE energies are shown in Fig. 4 (compound 4) where the CB-bottom is mainly formed by the Bi^{2+} ground state orbitals and the VB-top has mixed oxygen and Bi^{3+} character [34]. Such VRBE location is then consistent with a D-band type of charge transfer emission. However, the situation with $Bi_4Ge_3O_{12}$ remains complicated. What we do not know is the precise nature of the initial and final states and how lattice relaxation plays a role. It remains an unsolved problem to precisely characterize the transition in $Bi_4Ge_3O_{12}$. This cannot be answered by VRBE schemes alone.

3.5. The high efficiency of Sb^{3+} emission in $Ca_5(PO_4)_3(F,Cl)$

Sb^{3+} has $5s^2$ electron configuration and the ground and excited state energy levels are similar as those in the $6s^2$ element Bi^{3+}. The unsolved problem of Blasse relates to explaining the high room temperature quantum efficiency of the Sb^{3+} emission despite its 19000 cm^{-1} large Stokes shift. In the standard model of emission quenching via the crossing point between ground state and excited state parabolas in the configurational coordinate diagram (CCD), the Stokes shift, the width of emission and excitation bands, and thermal quenching temperature T_{50} are related properties. A low quenching temperature is, according to Blasse, then to be expected for Sb^{3+} emission in $Ca_5(PO_4)_3(F,Cl)$. Blasse and coworkers [35–37] speculated on an off-center position of Sb^{3+} on the Ca^{2+} site due to the small ionic radius of Sb^{3+}. In the excited state it moves on-center and such movement entails a large offset in the configuration coordinate diagram and hence large Stokes shift. There are two aspects here to consider (1) quenching need not to proceed via the crossing point in the CCD but may also proceed via electron ionization to the CB or hole ionization to the VB. (2) lattice relaxation may change the site symmetry and crystal field splitting in the excited state.

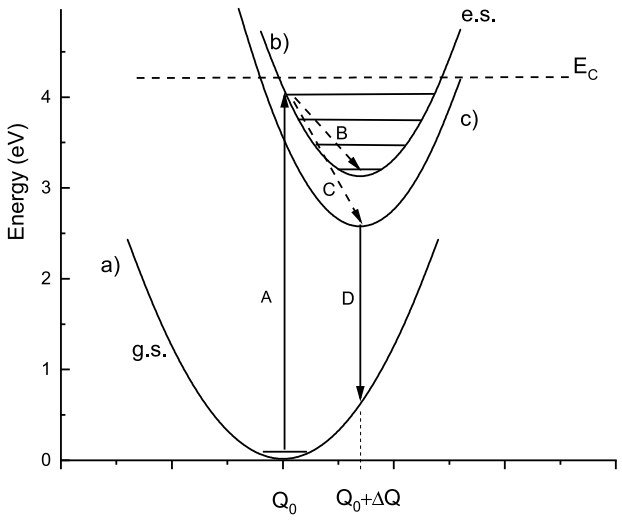

Fig. 5. Configurational coordinate diagram to illustrate that a large Stokes shift and high quenching temperature not necessarily contradict each other.

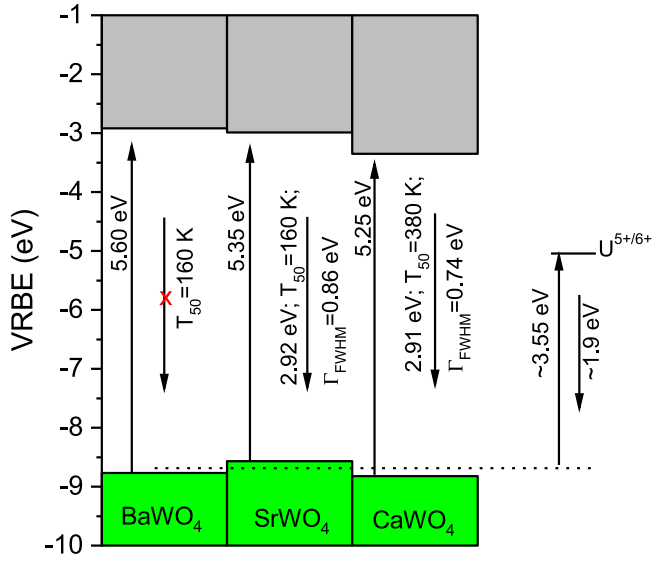

Fig. 6. A stacked diagram showing the VRBEs at the VB-top and the CB-bottom of $BaWO_4$, $SrWO_4$, and $CaWO_4$ where in each case a U-value of 7.1 eV was used. Energy of host exciton creation at 10 K and WO_4^{2-} emission together with the T_{50} quenching temperature and the width of the emission band are provided. The $U^{5+/6+}$ charge transition level is placed at −5.2 eV.

The situation for Ce^{3+} on the La^{3+} site in $NaLaF_3$, $LaCl_3$ and $LaBr_3$ is illustrated with the configuration coordinate diagram sketched in Fig. 5. The 5d-4f emission of Ce^{3+} is strongly Stokes shifted but still the quenching temperature is high, see Fig. 3. In Fig. 5 the excited state parabola (b) is offset by ΔQ from the ground state parabola (a). If quenching proceeds via ionization to the CB and ΔQ increases, the Stokes shift and band width will increase as usual but the quenching temperature T_{50} will remain the same. So, a large Stokes shift not necessarily implies a low quenching temperature. There is yet another aspect. The coordination around the La-site in $NaLaF_3$, $LaCl_3$ and $LaBr_3$ is 9-fold in the form of a tri-capped trigonal prism and Ce^{3+} is in its ground state on-center located. With such 9-fold coordination, crystal field splitting of the 5d-levels is relatively small. A cluster calculation on the lattice relaxation in the Ce^{3+} ground and excited state provided answers to the lattice relaxation dynamics [38]. Upon excitation to the 5d-state, one anion moves outward and the other eight inward and in addition the Ce^{3+} moves off-center. Effectively the coordination around Ce^{3+} is changed from 9-fold to 8-fold in the form of a square antiprism. Such type of coordination enhances crystal field splitting of the 5d-levels. The $5d_1$ excited state parabola is then not only offset but also lowered in energy as illustrated with parabola (c) in Fig. 5. The energy lowering will appear in the Stokes shift. In this case a large Stokes shift not necessarily implies a low quenching temperature it also not necessarily implies wide emission and excitation bands. On the contrary, the enlarged Stokes shift moves the excited state further below E_C and quenching temperature increases.

Returning to the exceptionally large Stokes shift for the Sb^{3+} emission in $Ca_5(PO_4)_3(F,Cl)$. To solve Blasse's problem one should not just consider the standard configurational coordinate offset interpretation. First one needs to establish whether quenching proceeds via the crossing point in the CCD, or via electron ionization to the CB, or via hole ionization to the VB. Information on the VRBEs in the Sb^{3+} states is then required. However, a systematic study on Sb^{3+} VRBEs has not been performed yet, and the issue remains therefore open.

3.6. The quenching temperature of the WO_4^{2-} and the uranate emission

The quenching temperature T_{50} of the WO_4^{2-} emission in the series $CaWO_4$, $SrWO_4$, $BaWO_4$ decreases from 380 K to 160 K to 0 K, respectively [1]. It was proposed that the increasing size of the alkaline earth (AE) cation softens the lattice which allows a larger offset in the configuration coordinate diagram which in turns results in higher probability of the nonradiative transitions. With such explanation one also expects larger Stokes shift and wider emission bands. Fig. 6 shows the VRBE schemes for these three tungstates [14]. Indeed the full width at half maximum emission intensity (Γ_{FWHM}) for $CaWO_4$ appears as expected somewhat smaller than for $SrWO_4$ but the Stokes shift for $CaWO_4$ appears slightly larger. Although errors in VRBE energies can be several 0.1 eV, the several 0.1 eV lowering of the VRBE at the CB-bottom with smaller size of the alkaline earth is genuine. It is also observed in vanadates, titanates, tantalates, molybdates, and niobates [14]. The CB-bottom in these compounds is formed by the lowest energy d-orbital of the transition metal. With smaller AE size, the lattice parameter decreases resulting in a larger crystal field splitting between the 3d, 4d, and 5d CB-levels and consequently lower lying CB-bottom. These VRBE diagrams, like for YVO_4, can explain the quenching temperature of Tb^{3+} and Pr^{3+} 4f-4f emissions, they also explain the absence of Ce^{3+} 5d-4f emission, however, they cannot explain the change of WO_4^{2-} quenching temperature, and that issue will remain unsolved.

A final issue is the changing quenching temperature of the uranate emission in $CaWO_4$ (645 nm), $SrWO_4$ (660 nm), and $BaWO_4$ (660 nm) that increases from 123 K to 290 K to 410 K [1]. The luminescence of U^{6+} and for that matter other actinides has received very little attention past 25 years. A study on the location of the actinide levels within the band gap of materials has also not been conducted. U^{6+} has an unfilled 5f orbital and emission and excitation spectra in the three tungstate compounds can be found in 't Lam et al. [39]. In all three compounds the first excitation band appears around 350 nm (3.55 eV). Likely this is related with electron transfer from the valence band to U^{6+}, and this would located the U^{5+} ground state level (or $U^{5+/6+}$ charge transition level) about 3.55 eV above the valence band top, i.e., near −5.2 eV. Highest energy emission for all three compounds is near 650 nm (1.91 eV) which implies about 1.6 eV Stokes shift consistent with a charge transfer type of luminescence phenomenon. Due to limited accuracy of VRBE schemes and because lattice relaxation effects are not accounted for, an explanation for the changing quenching temperature cannot be provided. Blasse's problem remains unsolved.

4. Summary and conclusions

Blasse's unsolved problems of 1997 all relate to electron transfer phenomena, and in cases of electron transfer the electron binding energy in the initial and final states are important. VRBE diagrams constructed with the refined chemical shift model provide information on binding energies in lanthanide, Bi^{3+}, Bi^{2+}, Pb^{2+} impurity states and at the VB-top and CB-bottom. The quenching temperature of Tb^{3+} $^5D_4$ and $^5D_3$ emission are well-explained with VRBE diagrams as demonstrated for YVO_4 in Fig. 2 but also in many other compounds. The same applies for the quenching temperature of Ce^{3+} 5d-4f emission and absence of such emission in the sesqui-oxides as illustrated in Fig. 3. Also the yellow emission of Bi^{3+} in YVO_4, or more generally the charge transfer emissions involving Bi^{3+} and Pb^{2+}, and the issues related with Bi^{2+} can all be well-addressed with VRBE scheme construction.

There are still many unresolved problems, particularly regarding the quenching temperature of emission. Quenching temperature is very sensitive to the value of the quenching energy barrier. It changes typically 500–1000 K/eV. VRBE schemes can explain quenching when it proceeds by electron transfer to the CB, however since accuracy is at most few 0.1 eV, that already creates uncertainty of several 100 K in predicting T_{50} quenching temperature. Charge transfer between different atoms is always followed by quite substantial lattice relaxation resulting in large (1–2 eV) Stokes shifts between excitation and emission. This is something that VRBE diagrams cannot deal with. Explaining the quenching temperature quantitatively we need 'the hope' that is still contained in Pandora's box.

Declaration of competing interest

The authors declare that they have no known competing financial interests or personal relationships that could have appeared to influence the work reported in this paper.

References

[1] G. Blasse, J. Lumin. 72–74 (1997) 129.
[2] P. Dorenbos, Phys. Rev. B 85 (2012) 165107.
[3] P. Dorenbos, J. Lumin. 214 (2019) 116536.
[4] P. Dorenbos, J. Lumin. 222 (2020) 117164.
[5] P. Dorenbos, Phys. Rev. B 87 (2013) 035118.
[6] R.H.P. Awater, P. Dorenbos, J. Lumin. 184 (2017) 221.
[7] R.H.P. Awater, P. Dorenbos, J. Lumin. 192 (2017) 783.
[8] E.G. Rogers, P. Dorenbos, ECS J. Sol. State Sci. Technol. 3 (2014) R173.
[9] J. Ueda, A. Hashimoto, S. Takemur, K. Ogasawara, P. Dorenbos, S. Tanabe, J. Lumin. 192 (2017) 371.
[10] Bingyan Qu, Rulong Zhou, Lei Wang, Pieter Dorenbos, J. Mater. Chem. C 7 (2019) 95.
[11] P. Dorenbos, J. Lumin. 136 (2013) 122.
[12] P. Boutinaud, R. Mahiou, E. Cavalli, M. Bettinelli, Chem. Phys. Lett. 418 (2006) 185.
[13] P. Boutinaud, P. Putaj, R. Mahiou, E. Cavalli, A. Speghini, Spectrosc. Lett. 40 (2007) 209.
[14] P. Dorenbos, E.G. Rogers, ECS J. Solid State Sci. Technol. 3 (2014) R150.
[15] M. Raukas, S.A. Basun, W. van Schaik, W.M. Yen, U. Happek, Appl. Phys. Lett. 69 (1996) 3300.
[16] Y. Shen, D.B. Gatch, U.R. Rodriguez Mendoza, G. Cunningham, R.S. Meltzer, W.M. Yen, K.L. Bray, Phys. Rev. B 65 (2002) 212103.
[17] M.A. Hamstra, H.F. Folkerts, G. Blasse, J. Mater. Chem. 4 (1994) 1349.
[18] Hong-Tao Sun, Jiajia Zhou, Jianrong Qiu, Prog. Mater. Sci. 64 (2014) 1.
[19] Y. Katayama, A. Hashimoto, Jian Xu, J. Ueda, S. Tanabe, J. Lumin. 183 (2017) 355.
[20] Tianshuai Lyu, Pieter Dorenbos, J. Mater. Chem. C 6 (2018) 6240.
[21] T. Lyu, P. Dorenbos, Chem. Mater. 32 (2020) 1192.
[22] Y. Katayama, J. Ueda, S. Tanabe, Opt. Mater. Expr. 4 (2014) 613.
[23] R.H.P. Awater, P. Dorenbos, J. Lumin. 188 (2017) 487.
[24] R.H.P. Awater, L.C. Niemeijer-Berghuijs, P. Dorenbos, Opt. Mater. 66 (2017) 351.
[25] R.T. Poole, J. Liesegang, R.C.G. Leckey, J.G. Jenkin, J.B. Peel, Phys. Rev. B 13 (1976) 896.
[26] M. Back, J. Ueda, E. Ambrosi, L. Cassandro, D. Cristofori, R. Ottini, P. Riello, G. Sponchia, K. Asami, S. Tanabe, E. Trave, Chem. Mater. 31 (2019) 8504.
[27] Shujuam Zhang, Yuguo Yang, J. Electron. Mater. 43 (2014) 389.
[28] Z. Grubac, J. Katic, M. Metikos-Hukovic, J. Electrochem. Soc. 166 (2019) H433.
[29] J. Morasch, Shunyi Li, J. Brotz, W. Jaegermann, A. Klein, Phys. Status Solidi A 211 (2014) 93.
[30] Xinping Lin, Jingcheng Xing, Wendeng Wang, Zhichao Shan, Fangfang Xu, Fuqiang Huang, Phys. Chem. C 111 (2007) 18288.
[31] Shuxing Wu, Jianzhang Fang, Weicheng Xu, Chaoping Cen, J Chem. Technol. Biotechnol. 88 (2013) 1828.
[32] G. Boulon, J. Phys. (Paris) 32 (1971) 333.
[33] A. Krasnikov, V. Tsiumra, L. Vasylechko, S. Zazubovich, Ya Zhydachevskyy, J. Lumin. 212 (2019) 52.
[34] M. Itoh, T. Katagiri, H. Mitani, M. Fujita, Y. Usuki, Phys. Stat. Sol. (B) 245 (2008) 2733.
[35] E.W.J.L. Oomen, G.J. Dirksen, W.M.A. Smit, G. Blasse, J. Phys. C: Solid State Phys. 20 (1987) 1161.
[36] E.W.J.L. Oomen, W.M.A. Smit, G. Blasse, Mater. chem. phys., 19 (1988) 351.
[37] L.i van Steensel, G. Blasse, J. Alloys Compd. 232 (1996) 60.
[38] J. Andriessen, E. van der Kolk, P. Dorenbos, Phys. Rev. B 76 (2007) 075124.
[39] R.U.E. 't Lam, G. Blasse, J. Chem. Phys. 72 (1980) 1803.